Journal of Applied Mechanics and Technical Physics, Vol. 42, No. 6, pp. 1057–1063, 2001

NUMERICAL ANALYSIS OF AXISYMMETRIC BUCKLING OF CONICAL SHELLS

L. I. Shkutin

UDC 539.370

Nonlinear boundary-value problems of axisymmetric buckling of conical shells under a uniformly distributed normal pressure are solved by the shooting method. The problems are formulated for a system of six first-order ordinary differential equations with independent rotation and displacement fields. Simply supported and clamped cases are considered. Branching solutions of the boundary-value problems are studied for different pressures and geometrical parameters of the shells. The nonmonotonic and discontinuous curves of equilibrium states obtained show that collapse, i.e., snap-through instability is possible. For a simply supported shell, multivalued solutions are obtained for both external and internal pressure. For a clamped thin-walled shell, theoretical results are compared with experimental data.

The earliest analysis of nonlinear deformation of shallow spherical domes was given in [1, 2], and many theoretical and experimental studies have been performed in this direction ever since. The cases of a central point force and normal pressure distributed over the entire surface of a dome or over a part of it were considered. Results of these studies are briefly reviewed in [3]. Numerical analysis was performed within the framework of the nonlinear model of shallow shells [4, 5]. To solve nonlinear boundary-value problems of axisymmetric deformation of a dome, the step-by-step (with respect to the loading parameter) method was employed. This method is used to find solutions branching from the basic one, which requires special techniques for constructing solutions in the neighborhood of the bifurcation point. Therefore, it is difficult to obtain isolated solutions characteristic of nonlinear problems of deformation of bars, plates, and shells. An exception is the work of Feodos'ev [6] who solved the problem of nonlinear deformation of a clamped spherical dome loaded by a uniformly distributed pressure by the shooting method. The author [7, 8] employed this method to analyze the branched shapes of bars and arches in bending.

In the present paper, we use the shooting method to solve the boundary-value problems of axisymmetric buckling of a conical dome, which is difficult to analyze because of the pointed apex. The nonlinear boundary-value problems are formulated within the framework of the mathematical model of deformable shells with independent fields of finite displacements and rotations [9, 10].

System of Equations. We consider a dome-like shell with an axisymmetric base surface A. On the surface, we introduce a curvilinear coordinate system t_J with a local orthonormal basis $\boldsymbol{a}_J(t_1, t_2)$ $(J = 1, 2, 3)$. The parameters $t_1 \equiv t \in [0, 1]$, $t_2 \in [0, 2\pi]$, and $t_3 \in [-h, h]$ are reckoned along the meridian, parallel, and normal to the surface, respectively ($2h$ is the thickness of the dome). We also introduce a cylindrical coordinate system (y, t_2, z) with an orthonormal basis $\boldsymbol{e}_J(t_2)$. The surface basis is obtained from the cylindrical basis by rotation through the angle $\theta_2(t)$ about the vector $\boldsymbol{e}_2$. In this case, $\boldsymbol{a}_2 = \boldsymbol{e}_2$ and the positive direction of $\boldsymbol{e}_2$ and the positive value of the angle are determined by the right-hand rule. The rotation transformation is given by the matrix

$$\Theta_2 = \begin{pmatrix} \cos\theta_2 & 0 & \sin\theta_2 \\ 0 & 1 & 0 \\ -\sin\theta_2 & 0 & \cos\theta_2 \end{pmatrix}.$$

Institute of Computer Modeling, Siberian Division, Russian Academy of Sciences, Krasnoyarsk 630090.
Translated from Prikladnaya Mekhanika i Tekhnicheskaya Fizika, Vol. 42, No. 6, pp. 159–165, November–December, 2001. Original article submitted April 3, 2001; revision submitted July 9, 2001.

0021-8944/01/4206-1057 $25.00

In the initial (stress-free) state, the meridian of the dome is defined by the parametric equations

$$y = r_2(t), \qquad z = r_3(t), \qquad \theta = \theta_2(t) \qquad \forall t \in [0,1]. \tag{1}$$

By definition, we have the relations $dr_2/ds_1 = \cos\theta_2$, $dr_3/ds_1 = -\sin\theta_2$, $ds_1 = l\,dt$, and $ds_2 = r_2\,dt_2$, where ds_1 and ds_2 are the elementary arcs of the meridian and parallel, respectively, and l is the length of the meridian.

We consider the axisymmetric deformation of the dome, for which the base surface remains axisymmetric and is defined by equations similar to (1)

$$y = z_2(t), \qquad z = z_3(t), \qquad \theta = \theta(t) \qquad \forall t \in [0,1],$$

where z_2 and z_3 are unknown cylindrical coordinates of a point and θ is the sought angle of rotation of the local basis relative to the cylindrical one. The matrix

$$\Theta = \begin{pmatrix} \cos\theta & 0 & \sin\theta \\ 0 & 1 & 0 \\ -\sin\theta & 0 & \cos\theta \end{pmatrix}$$

transforms the cylindrical basis $\boldsymbol{e}_J$ to the rotated basis $\boldsymbol{a}_J^0 = \Theta \cdot \boldsymbol{e}_J$.

To analyze the axisymmetric deformation of the dome, we use the equations of the nonlinear model of a deformable shell with independent finite displacements and rotations [9, 10]. The material of the dome is assumed to be isotropic and linearly elastic.

The initial system of equations comprises

— the moment relations

$$\begin{gathered} U_{11} = (1-\nu^2)F^{-1}X_{11} - \nu U_{22}, \qquad V_{11} = (1-\nu^2)H^{-1}Y_{11} - \nu V_{22}, \\ U_{13} = \gamma F^{-1}X_{13}, \qquad X_{22} = \nu X_{11} + FU_{22}, \qquad Y_{22} = \nu Y_{11} + HV_{22}, \end{gathered} \tag{2}$$

which follow from (2.9) in [10];

— the kinematic relations

$$\begin{gathered} V_{11} = (\theta - \theta_2)', \qquad V_{22} = r_2^{-1}(\sin\theta - \sin\theta_2), \qquad U_{22} = r_2^{-1}(z_2 - r_2), \\ z_2' = (1+U_{11})\cos\theta + U_{13}\sin\theta, \qquad z_3' = -(1+U_{11})\sin\theta + U_{13}\cos\theta, \end{gathered} \tag{3}$$

which follow from (1.6) in [10];

— the static equations

$$\begin{gathered} (r_2X_1)' - X_{22} + r_2P_1 = 0, \qquad (r_2X_3)' + r_2P_3 = 0, \\ (r_2Y_{11})' - Y_{22}\cos\theta - r_2X_{13} + r_2Q_2 = 0, \\ X_{11} = X_1\cos\theta - X_3\sin\theta, \qquad X_{13} = X_1\sin\theta + X_3\cos\theta, \end{gathered} \tag{4}$$

which follow from (1.7) in [10]. In system (2)–(4), $F = 2hE$, $3H = 2h^3E$, $\gamma = 2(1+\nu)$, E is Young's modulus, ν is Poisson's ratio, $U_{iJ}(t)$, $V_{ii}(t)$, $X_{iJ}(t)$, and $Y_{ii}(t)$ are the components of the metric and flexural strains, forces, and moments in the rotated basis, $X_1(t)$, $X_3(t)$, $P_1(t)$, $P_3(t)$, and $Q_2(t)$ are the components of the forces, surface loads, and moments in the cylindrical basis; the prime denotes differentiation with respect to s_1; $i = 1,2$. Equations (2) and the first three equations in (3) are formulated in the rotated basis, whereas Eqs. (4) and the last two equations in (3) are formulated in the cylindrical basis.

System (2)–(4) can be written in the form

$$
\begin{aligned}
&y_0' = \theta_2' + x^{-1}[(1-\nu^2)y_1 - \nu(\sin y_0 - \sin\theta_2)],\\
&y_1' = x^{-1}(\nu y_1 + \sin y_0 - \sin\theta_2)\cos y_0 + \varepsilon^{-1} y_7 - x q_2,\\
&y_2' = \varepsilon\gamma x^{-1} y_7 \sin y_0 + (1+y_8)\cos y_0,\\
&y_3' = \varepsilon\gamma x^{-1} y_7 \cos y_0 - (1+y_8)\sin y_0,\\
&y_4' = x^{-1}[\nu y_6 + \varepsilon^{-1}(y_2 - x)] - x p_1,\\
&y_5' = -x p_3,
\end{aligned} \tag{5}
$$

$$
y_6 = y_4\cos y_0 - y_5 \sin y_0, \quad y_7 = y_4 \sin y_0 + y_5\cos y_0, \quad y_8 = x^{-1}[(1-\nu^2)\varepsilon y_6 - \nu(y_2 - x)],
$$

where $y_0 = \theta$, $y_1 = xY_{11}l/H$, $y_2 = z_2/l$, $y_3 = z_3/l$, $y_4 = xX_1/C$, and $y_5 = xX_3/C$ are unknown functions, $\varepsilon^2 = h^2/(3l^2)$, $C = \varepsilon F$, $p_J = P_J l/C$, $q_2 = Q_2 l^2/H$, and $x = r_2/l$ are parameters; the prime denotes differentiation with respect to the independent variable t.

System (5) describes the nonlinear axisymmetric bending of a dome-like shell for given loading parameters p_1, p_3, and q_2 and rigidity parameters ε, γ, and ν under boundary conditions specified on the support contour. It is singular with respect to t (at the point $t = 0$) and the small parameter ε. We consider numerical solutions of two nonlinear boundary-value problems of axisymmetric bending of simply supported and clamped conical domes.

Simply Supported Conical Dome Under Normal Pressure. The initial shape of the dome is determined by the constant parameters h and l and the angle between the meridian and base plane α. The parameters l and α determine the height of the dome $a = l\sin\alpha$ and the radius of the support contour $b = l\cos\alpha$. Functions (1) have the form $\theta_2 = \alpha$, $r_3 = a(1-t)$, and $r_2 = bt$, and, hence, $x = t\cos\alpha$.

The dome is subjected to a uniformly distributed normal pressure of intensity P per unit area of the undeformed base surface. The components of the surface load in system (5) are determined by the functions $p_1 = -p\sin y_0$, $p_3 = -p\cos y_0$, and $q_2 = 0$, where $p = Pl/C$ is the normalized pressure parameter, which is positive for the external pressure. In the case of a simply supported contour, the moment and displacements vanish at the boundary point $t = 1$:

$$
y_1(1) = 0, \qquad y_2(1) = \cos\alpha, \qquad y_3(1) = 0. \tag{6}
$$

At the pole $t = 0$, we specify the symmetry conditions

$$
y_0(0) = \alpha, \qquad y_2(0) = 0, \qquad [t^{-1} y_5(t)]_{t\to 0} \to 0. \tag{7}
$$

The nonlinear boundary-value problem (5)–(7) was solved by the shooting method: at the point $t = 1$, in addition to (6), we specified three conditions

$$
y_0(1) = k_1, \qquad y_4(1) = k_2, \qquad y_5(1) = k_3 \tag{8}
$$

and varied the parameters k_J to construct numerically a three-parameter family of solutions $\boldsymbol{y}(t, k_J)$ of the one-point problem (5), (6), (8) ($\boldsymbol{y}$ is the vector of unknown functions). The values of the varied parameters corresponding to the solution of the initial boundary-value problem were determined by an iterative method with the use of three conditions (7) specified at the point $t = 0$. In practice, however, this method is ineffective because of the instability associated with the presence of pole singularities in system (5). A solution stable with respect to small perturbations of the boundary parameters was obtained by a modified algorithm in which the approximate relations $X_{22} \approx X_{11}$, $Y_{22} \approx Y_{11}$, and $y_5 \approx (1/2)p\delta^2\cos^2\alpha$ were used at the point $t = \delta$ close to the pole. The first two relations are exact at the pole. The third relation is obtained by integrating the last equation in (5) over the interval $[0, \delta]$ for $y_0 = \alpha$. The calculations were performed with the use of the Mathcad-7 software package.

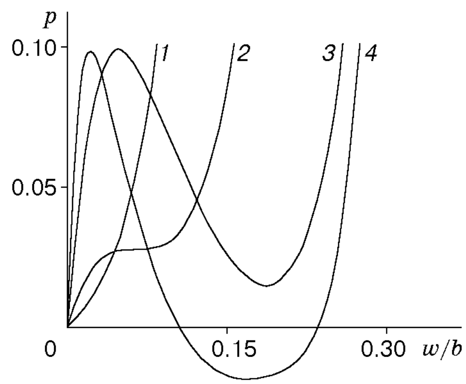

Fig 1

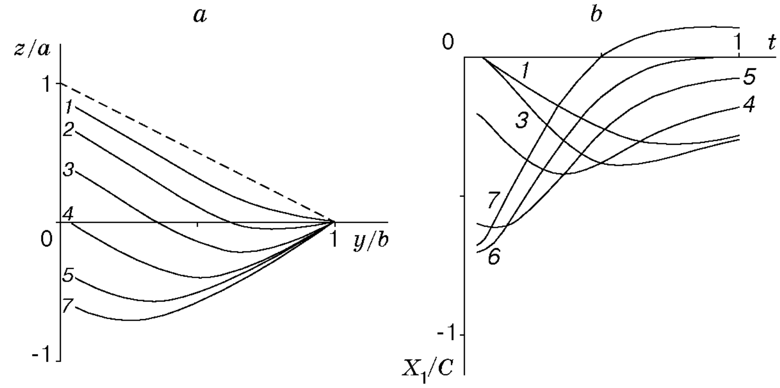

Fig. 2

Fig. 1. Curves of equilibrium states for simply supported shells: curve 1 refers to $\alpha = 0$ and $\varepsilon = 0.025$, curve 2 to $\alpha = \pi/36$ and $\varepsilon = 0.025$, curve 3 to $\alpha = \pi/18$ and $\varepsilon = 0.025$, and curve 4 to $\alpha = \pi/18$ and $\varepsilon = 0.013$.

Fig. 2. Bending modes (a) and radial forces (b) of a dome with the parameters $\alpha = \pi/18$ and $\varepsilon = 0.013$ for points $(p; w/a) = (0.09; 0.0786)$ (1), $(0.06; 0.293)$ (2), $(0; 0.590)$ (3), $(-0.02; 0.968)$ (4), $(0; 1.338)$ (5), $(0.04; 1.469)$ (6), and $(0.1; 1.557)$ (7); the dashed curve is the initial configuration.

Figure 1 shows the curves of equilibrium states $p(w/b)$ (w is the axial displacement of the apex) of the dome with the rigidity parameters $\gamma = 2.5$ and $\nu = 0.25$ and various values of the geometrical parameters α and ε. Curve 1 refers to a simply supported circular plate. For $\varepsilon = 0.025$ and $0 \leqslant \alpha \leqslant \pi/36$, the curves are monotonic. For $\alpha > \pi/36$, curves 3 and 4 have extremes, which shows that the solution of the boundary-value problem (5)–(7) is multivalued within the finite interval $p^- \leqslant p \leqslant p^+$, where p^- and p^+ are the minimum and maximum values of the function $p(w/b)$, respectively. The states (shapes or modes) of equilibrium corresponding to the sections of the curves that ascend from the coordinate origin are called the basic states and other states are called the buckled states. For perfectly elastic domes, the basic states exist in the semi-infinite interval $-\infty < p \leqslant p^+$ (sections of the curves corresponding to the internal pressure $p < 0$ are not shown in Fig. 1). Curve 4 shows that, as the dome thickness decreases, the buckled modes occur for negative values of the loading parameter.

Figure 2a shows the equilibrium configurations of the dome with the geometrical parameters $\alpha = \pi/18$ and $\varepsilon = 0.013$ in the coordinates $(y/b, z/a)$ and Fig. 2b shows the distributions of the radial force calculated at several points $(p; w/a)$. The dashed curve is the initial configuration, curve 1 is the basic mode for the value of p close to the critical value $p^+ \approx 0.098$, and curves 2–7 are the buckled modes. Mode 4 corresponds to the negative value of p and modes 3 and 5 corresponding to the value $p = 0$ are stressed (in contrast to the initial state of the dome) and sustained in equilibrium by the radial support force $X_1(1)$.

Clamped Conical Dome Under Normal Pressure. In contrast to (6), the boundary conditions of a dome with a clamped support contour (displacements and rotations are absent) have the form

$$y_0(1) = \alpha, \qquad y_2(1) = \cos\alpha, \qquad y_3(1) = 0. \tag{9}$$

Figures 3 and 4 show the numerical solution of the nonlinear boundary-value problem (5), (7), (9) for clamped domes characterized by the same parameters as the simply supported domes considered above.

Figure 3 shows the curves of equilibrium states of the domes. Curve 1 refers to a clamped circular plate. The behavior of curves 3 and 4 shows that the buckled states of equilibrium exist only for positive values of the parameter p and no other states than the stress-free state exist for $p = 0$. Figure 4a shows the equilibrium configurations of the dome with the parameters $\alpha = \pi/18$ and $\varepsilon = 0.013$ and Fig. 4b shows the distributions of the radial forces calculated at some points $(p; w/a)$: curve 1 is the basic mode for the value of p close to the critical value $p^+ \approx 0.218$ and curves 2–7 are the buckled modes.

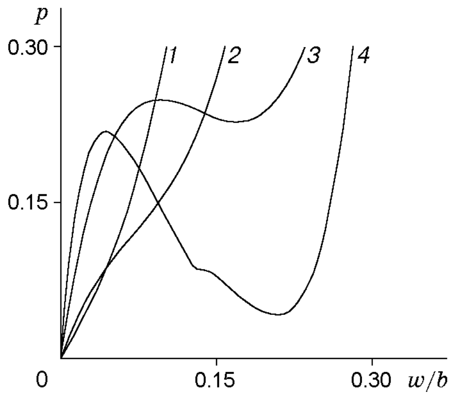

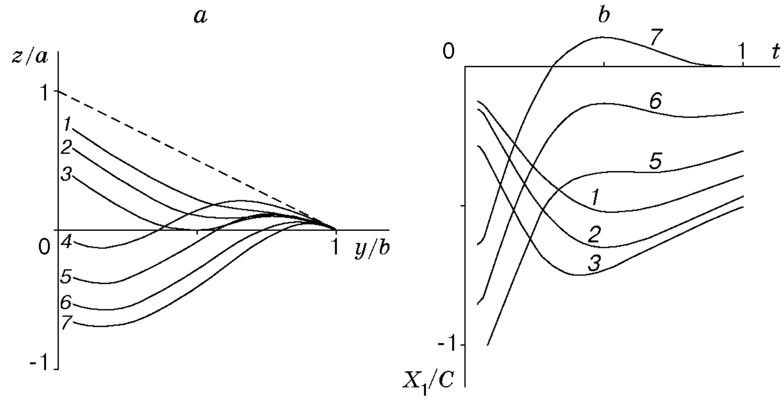

Fig. 3

Fig. 4

Fig. 3. Curves of equilibrium states for clamped shells: curve 1 refers to $\alpha = 0$ and $\varepsilon = 0.025$, curve 2 to $\alpha = \pi/36$ and $\varepsilon = 0.025$, curve 3 to $\alpha = \pi/18$ and $\varepsilon = 0.025$, and curve 4 to $\alpha = \pi/18$ and $\varepsilon = 0.013$.

Fig. 4. Bending modes (a) and radial forces (b) of a clamped dome with the parameters $\alpha = \pi/18$, and $\varepsilon = 0.013$ for points $(p; w/a) = (0.217; 0.230)$ (1), $(0.2; 0.366)$ (2), $(0.14; 0.558)$ (3), $(0.05; 1.034)$ (4), $(0.05; 1.296)$ (5), $(0.15; 1.484)$ (6), and $(0.3; 1.604)$ (7); the dashed curve is the initial configuration.

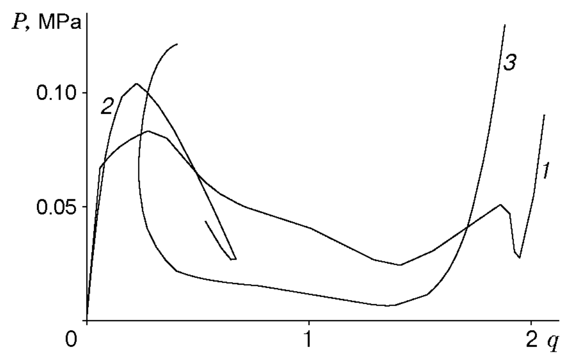

Fig. 5. Experimental (1) and theoretical (2 and 3) curves of equilibrium states of the dome with the parameters $\alpha = \pi/36$ and $\varepsilon = 0.0025$.

To compare numerical results with the experimental data of [11], we calculated a clamped conical dome with the parameters $\alpha = \pi/36$, $\gamma = 2.7$, $\varepsilon = 0.0025$, and $\nu = 0.35$. In the experiments, these data correspond to a copper conical shell of thickness $2h = 0.6$ mm, base diameter $2b = 138$ mm, and Young's modulus $E \approx 10^5$ MPa. Figure 5 shows the experimental data and calculation results in the coordinates (q, P) (P is the pressure in MPa and q is the parameter of state determined as the ratio of the volume enclosed between the undeformed and deformed surfaces of the dome to the initial volume of the dome). Curve 1 refers to the experimental dependence $P(q)$ and curves 2 and 3 to calculations. One can see that the calculated curve is branched. Intersection of branches 2 and 3 determines the bifurcation of the axisymmetric states of equilibrium of the dome in the calculations.

Figure 6a shows the calculated equilibrium configurations and Fig. 6b shows the experimental distributions of the bending moments of the dome at several points $(p; q)$ of curves 2 and 3 (see Fig. 5): curve 1 is the basic mode for the value of p close to the upper critical value $p^+ \approx 0.0475$, curve 4 is the buckled mode the lower critical point of curve 3, and curves 3 and 5 are the buckled modes corresponding to the points lying at the left and right ascending sections of curve 3 above the upper critical point.

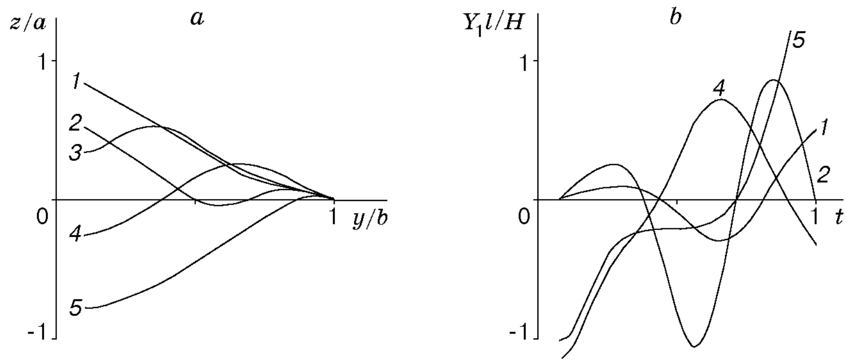

Fig. 6. Bending modes (a) and bending moments (b) of a clamped dome with the parameters $\alpha = \pi/36$ and $\varepsilon = 0.0025$ for points $(p; q) = (0.045; 0.302)$ (1), $(0.012; 0.667)$ (2), $(0.055; 0.365)$ (3), $(0.0028; 1.383)$ (4), and $(0.06; 1.87)$ (5).

The considerable discrepancy between the experimental and calculation results is caused by three factors.

1) The deformation of the experimental shell is close to axisymmetric up to the value $P \approx 0.068$ MPa, for which an intense wave formation (three waves) in the circumferential direction was observed, which corresponds to an abrupt change in the slope of the tangent below the maximum point (curve 1 in Fig. 5); nonsymmetric buckling occurred afterwards;

2) The deformation of the experimental shell was not completely elastic: when the load was removed, the shell remained in the snapped-through state and there was evidence of plastic strain along the support contour and at the crests of the circumferential waves;

3) The experimental curve of equilibrium states is discontinuous, since there are intervals of jumplike variation in pressure for small variation in volume (in the neighborhood of the point $q = 2$), which is the evidence of dynamic transitions from one state of equilibrium to another.

The first factor explains the discrepancy between the experimental and calculated curves in the neighborhood of the maximum point and in the interval where the function $P(q)$ decreases. The last two factors are responsible for the difference between the ascending sections of these curves in the neighborhood of the point $q = 2$.

Consequently, beginning from the value $q \approx 0.083$, the experimental and calculated curves in Fig. 5 correspond to different states of the dome: the first curve corresponds to the elastoplastic state oscillating along the circumferential coordinate, whereas the second curve corresponds to the elastic axisymmetric state. The agreement between the sections of these curves that ascend from the coordinate origin confirms the high accuracy of the formulation of the axisymmetric problem and the method of its solution.

The theoretical results are obtained under the assumption of a perfect linearly elastic material. The nonlinearities taken into account are of a kinematic character. A comparison with the experiment shows that precisely these nonlinearities determine the character of deformation of shells. Deviation from the linear-elastic behavior of the shell material leads only to quantitative changes in the characteristics of the process.

REFERENCES

1. C. B. Biezeno, "Uber die Bestimmung der "Durchschlagkraft" einer schwachgekrümmten, kreisformigen Platte," *Z. Angew. Math. Mech.*, **15**, 10–22 (1935).
2. T. Kármán and H. S. Tsien, "The buckling of spherical shells on external pressure," *J. Aeron. Sci.*, **7**, 43–50 (1939).
3. É. I. Grigolyuk and V. V. Kabanov, *Stability of Shells* [in Russian], Nauka, Moscow (1978).
4. K. Marguerre, "Zur Theorie der gekrümmten Platte grosser Formänderung," in: *Proc. of the 5th Int. Congress on Appl. Mech.* (Cambridge, 1938), J. Wiley and Sons, New York (1939), pp. 93–101.
5. V. Z. Vlasov, "Fundamental differential equations of the general theory of elastic shells," *Prikl. Mat. Mekh.*, **8**, No. 2, 109–140 (1944).

6. V. I. Feodos'ev, "A method of solving nonlinear problems of stability of deformable systems," *Prikl. Mat. Mekh.*, **27**, No. 2, 265–274 (1963).
7. L. I. Shkutin, "Numerical analysis of branching modes of bending of rods," *Prikl. Mekh. Tekh. Fiz.*, **42**, No. 2, 141–147 (2001).
8. L. I. Shkutin, "Numerical analysis of branching shapes of arches in bending," *Prikl. Mekh. Tekh. Fiz.*, **42**, No. 4, 155–160 (2001).
9. L. I. Shkutin, "Generalized models of the Cosserat type for finite deformation analysis of thin bodies," *Prikl. Mekh. Tekh. Fiz.*, **37**, No. 3, 120–132 (1996).
10. L. I. Shkutin, "Incremental deformation model for a shell," *Prikl. Mekh. Tekh. Fiz.*, **40**, No. 5, 202–207 (1999).
11. L. I. Shkutin and I. A. Shubin, "Experimental study of the stability of shallow conical shells under static pressure loads," *Prikl. Mekh.*, **2**, No. 6, 63–70 (1966).